Strong optical reflection of rare-earth garnets in the terahertz regime by reststrahlen bands

Masaki Adachi,[1,*] Hiroyasu Yamahara,[2] Shunsuke Kawabe,[2] Hiroaki Matsui,[1,2] and Hitoshi Tabata[1,2]

[1]*Department of Electrical Engineering and Information Systems, Graduate School of Engineering, University of Tokyo, 7-3-1 Hongo, Bunkyo-ku, Tokyo 113-8656, Japan*

[2]*Department of Bioengineering, Graduate School of Engineering, University of Tokyo, 7-3-1 Hongo, Bunkyo-ku, Tokyo 113-8656, Japan*

(Received 9 April 2014; revised manuscript received 11 May 2014; published 23 May 2014)

The reststrahlen bands of rare-earth garnets were investigated in the terahertz regime. Through this, it was found that the crystal orientation and light polarization directly influence the reststrahlen-related dielectric absorptions of $Gd_3Ga_5O_{12}$ (GGG), which is attributed to restriction in the vibrational motion of Gd ions. A theoretical fit to the dielectric absorption revealed that the phonon-polariton frequency in GGG crystals at around 85.5 cm^{-1} exhibits a narrow spectral width of 100 GHz at room temperature, as estimated using a Lorentz oscillator model. In addition, it was found that the reststrahlen bands can be readily manipulated within a range of 0.7–3.7 THz by changing the chemical composition of the garnet.

DOI: 10.1103/PhysRevB.89.205124 PACS number(s): 78.47.−p, 71.36.+c, 77.84.−s, 77.90.+k

I. INTRODUCTION

Since the invention of the optical-conducting antenna by Auston *et al.* [1] in 1984, basic and applied research into the terahertz (THz) regime (0.1–10 THz) has developed rapidly. These THz waves show great promise for future technology such as label-free biosensing, ultrafast telecommunications, and hazardous material inspection [2]. It is therefore of cardinal importance to understand the optical properties of such materials to ensure further progress in the creation of new optical devices based on this fast-growing frequency regime.

Through past research into optical elements, there has been a number of bandpass filters proposed based on a metallic mesh and metamaterial [3,4]. The spectral linewidth and frequency band of these filters can be freely controlled by altering the design of their periodic structure; however, their transmittance is ultimately determined by their aperture ratio. Consequently, a loss of transmitted power is essentially inevitable.

This problem can be overcome by the use of band-reflection devices, which allow for the reflection of a specific band of the THz wave with an efficiency of nearly 100%. This reflection phenomenon, well known as the reststrahlen band, is based on phonon-polariton interaction and is intimately associated with longitudinal-optical (LO) and transverse-optical (TO) phonons. Although this phonon-polariton band normally exists in the infrared regime, the phonon-polariton bands of certain dielectric oxides have been observed in the THz regime [5,6]. This means that the reststrahlen bands of these materials also exist in the THz regime, a sharp reststrahlen band being particularly evident when the respective frequencies of the TO and LO phonons are close. Recent vibrational simulations have reported interesting properties of rare-earth garnets in the THz regime [7], with the expectation that a sharp reststrahlen band will be found here.

Thus far, rare-earth garnets have received much attention as an optical material. For example, the incorporation of Nd^{3+} and Bi^{3+} ions into $Y_3Al_5O_{12}$ (YAG) is known to yield tunable solid-state lasers [8]. Furthermore, these ions can selectively target tetrahedral, octahedral, and dodecahedral cation sites in rare-earth garnets [Fig. 1(a)], thereby allowing for tuning of the laser oscillation frequency. This suggests that rare-earth garnets are of particular value in investigating sharp reststrahlen reflections, such reflection being readily controllable by varying the chemical composition. Moreover, if the correlation between the reststrahlen band and chemical composition can be determined, it has the potential to provide us an alternative to metallic mesh in the design of bandpass filters.

To this end, this study explores the effect of both rare-earth ions (R site) and metal ions (M site). In terms of the physics involved, an analysis of the chemical composition in the common space group provides a systematic understanding of the vibrational mode in the THz regime. It is important to note that this is true not only for the structure of garnet, but also any other lattice structure. From a practical engineering perspective, such analysis should provide an answer as to tune the sharp reststrahlen reflection to achieve a desired frequency. At the very least, the material that exhibits the desired spectroscopic character in the THz regime will be identified.

II. EXPERIMENT

Single crystals of $Gd_3Ga_5O_{12}$ (GGG), fabricated by a Czochralski method, were purchased from Crystal Base Co., Ltd. Polycrystalline samples of $Re_3Fe_5O_{12}$ (RIGs; Re = Y, Sm, Eu, Gd, Ho, and Lu) and $Re_3Ga_3O_{12}$ (RGGs; Re = Sm, Gd, and Ho) were synthesized by a solid-state reaction technique. The Re oxides (Re = Y, Sm, Eu, Gd, Ho, and Lu), Fe_2O_3, and Ga_2O_3 powders were mixed to obtain the desired starting compositions, and then pressed at 50 MPa in vacuum to form pellets. Next, these pellets were sintered at 1200 °C for 10 h in air (cooling rate: 10 °C/h), reground, and then fired again under the same sintering conditions. Finally, the sintered pellets were polished by lapping in order to obtain a mirror finish. All samples possessed a single phase with a garnet structure, as confirmed by x-ray diffraction.

Optical anisotropy was confirmed using GGG single crystals. The RIGs exhibit paraelectric and ferrimagnetic properties at room temperature (RT), whereas the RGGs have paraelectric and paramagnetic characters at the same

*Present address: 7-3-1 Hongo, Bunkyo-ku, Tokyo 113-8656, Japan; adachi@bioxide.t.u-tokyo.ac.jp

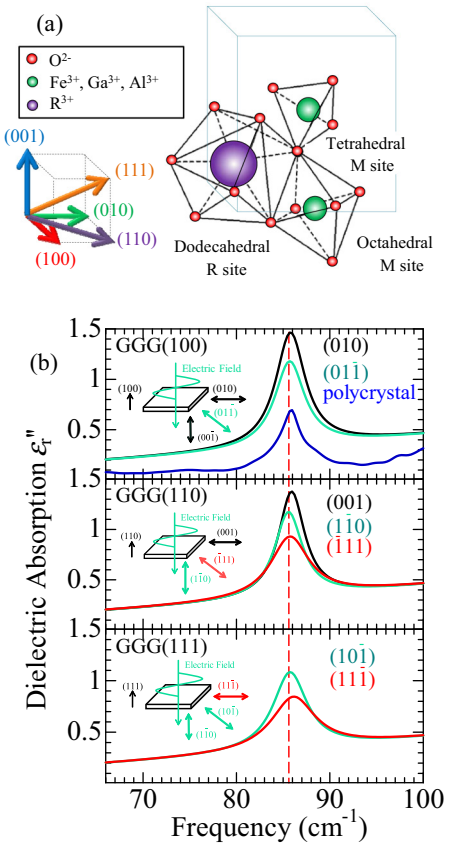

FIG. 1. (Color online) (a) Schematic structure of a rare-earth garnet with dodecahedrally coordinated *R* sites, and tetrahedrally and octahedrally coordinated *M* sites. (b) Dielectric absorption spectra of different azimuths on the (100), (110), and (111) surfaces of a GGG crystal and randomly oriented polycrystalline samples.

temperature. From previous reports [9,10], it is known that magnetic-related absorption is only found in RIGs and RGGs at low temperatures, and cannot be observed at RT. Consequently, light absorption peaks are considered the result of dielectric absorptions (ε_r'') when $\mu = 1+0i$, even in the case of the RIG samples (μ: the complex magnetic permeability). Dielectric absorptions were obtained using a transmittance-type terahertz time-domain spectroscope (THz-TDS: TAS7500SP, Advantest Co.), and are herein used as the basis for discussing the reststrahlen bands.

III. RESULTS AND DISCUSSION

Figure 1(b) shows the dielectric absorption spectra of the GGG crystals and polycrystalline samples at different azimuth configurations. From this, we see that the lowest phonon frequency mode of GGG is observed in the THz regime, as predicted by group theory [7]. These dielectric absorption peaks were theoretically fitted by a Lorentz oscillator model: $Aw^2/[4(\omega-\omega_0)^2+w^2]$; where ω_0 is the resonant frequency, A is the peak intensity, and w is the full width at half maximum (FWHM). This fitting is performed using two Lorentzian peaks—a sharp peak at 85.5 cm^{-1} and a broad peak at around 200 cm^{-1}. The broad peak results from a higher-frequency phonon, and thus the fitted parameters shown in Table I are for the sharp peak only.

TABLE I. Fitting parameters for a Lorentz oscillator model.

Sample	In-plane azimuth	Frequency (cm^{-1})	Peak value	FWHM (cm^{-1})
(110)	[010]	85.783	1.13	3.841
	[01–1]	85.693	0.854	3.894
(110)	[001]	85.898	1.04	3.432
	[0–10]	85.569	0.845	3.789
	[–111]	85.711	0.611	4.967
(111)	[10–1]	85.728	0.753	4.401
	[11–1]	86.093	0.512	5.704
Polycrystal		85.942	0.451	3.974

All of the dielectric absorption spectra exhibit sharp peak structures at around 85.5 cm^{-1}, which is indicative of TO and LO phonons. Thus, the peak frequency of the GGG crystal sample is close to those of the GGG polycrystalline samples [upper part in Fig. 1(b)]. Furthermore, the spectral linewidths of the single crystal and polycrystalline samples share a similar FWHM value within the resolution limit of 0.254 cm^{-1}. However, there is a notable difference in the peak intensity of the GGG crystal and polycrystalline samples. This can be explained by the multiple subgrains of the polycrystalline sample, the phonon coherence excited at 85.5 cm^{-1} being reduced in intensity by the random orientation of the grain boundaries. This is confirmed by the fact that the peak frequencies and spectral linewidths of the reststrahlen band are not sensitive to crystallinity.

In-plane polarization of the dielectric absorption was obtained on the (100), (110), and (111) surfaces of the GGG crystals. Since the isometric symmetry of garnets would ordinarily require optical isotropy, it is apparent that their complex permittivity is independent of optical polarization along the in-plane directions. The lowest optical phonon mode is related to the motion of rare-earth ions [7,10]. Using molecular dynamics (MD) theory, Papagelis *et al.* have previously calculated the partial density of state (DOS) and different atoms and for the total one-phonon density of state (PDOS) in garnets. These MD calculations indicated that approximately 90% of the total PDOS at the lowest phonon frequency contributes to the DOS of rare-earth ions [7]. Therefore, in the case of GGG, the dielectric absorptions are derived from vibrational motions ascribed to Gd ions. As shown in Fig. 1(b), only a slight frequency shift was observed for different polarization configurations. On the (110) surface, the peak positions were located at 85.898, 85.569, and 85.711 cm^{-1} along the [001], [1–10], and [–111] directions, respectively. The corresponding dielectric absorption values were approximately 1.04, 0.845, and 0.611, while the FWHMs were about 3.432, 3.789, and 4.967 cm^{-1}. Thus, in a single crystal, light absorption by phonon vibration is clearly affected by the direction of the electric field relative to the incident light. In this study, the incident direction of the THz electric field creates three distinct angles (θ: 65.9°, 30.0°, and 19.5°) for the vibrational direction of the nearest Gd-Gd ions, which explains the difference in dielectric absorption along the

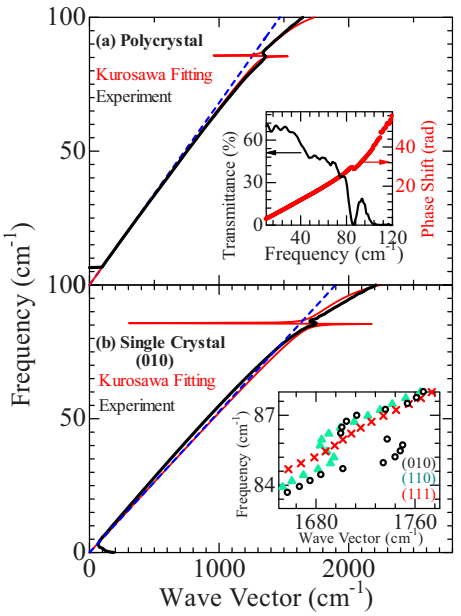

FIG. 2. (Color online) (a) Phonon-polariton dispersion curve of a GGG ceramic sample. The inset shows the dependence of transmittance (black line) and phase shift [red (gray) line] on frequency. (b) Phonon-polariton dispersion curve of a GGG crystal sample. The inset depicts the dependence of crystal orientation on the dispersion curve. The red (gray) line is fitted using Eqs. (1)–(4). The blue dotted line was determined by the relation $\omega = ck(\omega)/\sqrt{\varepsilon(0)}$, which was adopted to lower wave vectors below 500 cm^{-1}.

in-plane directions. In addition, the broadening of the peaks evident from the increase in FWHM, is most likely caused by damping due to the restricted motion of the Gd-Gd ions.

Figure 2 shows the phonon-polariton dispersions of GGG crystal and polycrystalline samples. The LO and TO phonon frequencies were estimated from experimental data using the Kurosawa formula, wherein the wave vector $k(\omega)$ of the phonon-polariton is calculated from the phase shift (φ); $\varphi = \{k(\omega)–\omega/c\}d$, where d is the sample thickness and c is the light velocity. The thicknesses of crystal and polycrystalline samples were 500 and 359 μm, respectively, and thus $\varepsilon(\omega)$ was described by the following expression [11]:

$$\frac{c^2k(\omega)^2}{\omega^2} = \varepsilon(\omega) = \prod_{i=1}^{N} \frac{\omega_{\mathrm{LO}i}^2 - \omega^2}{\omega_{\mathrm{TO}i}^2 - \omega^2}. \quad (1)$$

For low frequencies (i.e., less than 100 cm^{-1}), Eq. (1) was approximated as

$$k(\omega) = \frac{\sqrt{\varepsilon(1)}}{c}\omega \prod_{i=1}^{N} \left(\frac{\omega_{\mathrm{LO}i}^2 - \omega^2}{\omega_{\mathrm{TO}i}^2 - \omega^2}\right)^{1/2}, \quad (2)$$

$$\varepsilon(1) = \varepsilon(\infty)\omega \prod_{i=3}^{N} \frac{\omega_{\mathrm{LO}i}^2}{\omega_{\mathrm{TO}i}^2}, \quad (3)$$

where $\varepsilon(1)$ is considered the higher modes of $i > 3$ [6]. Furthermore, $\varepsilon(0)$ and $\varepsilon(\infty)$ can be determined by Eq. (3) and the Lyddane-Sachs-Teller (LST) relationship, as described by the following expression [12,13]:

$$\frac{\varepsilon(0)}{\varepsilon(\infty)} = \prod_{i=1}^{N} \frac{\omega_{\mathrm{LO}i}^2}{\omega_{\mathrm{TO}i}^2}. \quad (4)$$

TABLE II. Fitting parameters for Kurosawa formula.

Sample	[010]	[1–10]	[–111]	Polycrystal
$\omega_{\mathrm{TO1}}(cm^{-1})$	85.6	85.6	85.6	85.6
$\omega_{\mathrm{LO1}}(cm^{-1})$	85.7	85.7	85.7	85.65
$\omega_{\mathrm{TO2}}(cm^{-1})$	107.3	106.8	106.8	106.3
$\omega_{\mathrm{LO2}}(cm^{-1})$	105	108.9	109.7	108.9
$\varepsilon(\infty)$	3.6	3.6	3.6	3.6
$\varepsilon(1)$	12.23	12.31	12.12	7.5
$\varepsilon(0)$	12.8	12.83	12.82	7.881

Table II summarizes the fitted parameters, with the $\varepsilon(0)$ and $\varepsilon(\infty)$ values of the GGG crystal estimated at 12.8 and 3.6, respectively. These values are close to those previously reported for GGG crystals [$\varepsilon(0) = 12.1$ and $\varepsilon(\infty) = 3.49$] [14,15], which shows the validity of the theoretical calculations in the present analysis. The peak frequencies of the reststrahlen band between LO and TO phonons for all surface planes were all narrowly positioned within a range of 85.6–85.7 cm^{-1} [Table II]. On the other hand, the values of $\varepsilon(0)$ and $\varepsilon(\infty)$ for the polycrystalline sample were different from those of the single crystal samples, which is attributed to the small subgrains of the former. From Fig. 2 and Table II, it is clear that the peak frequencies of the TO and LO phonons remain unchanged in all samples. This indicates that the polycrystalline samples make full use of determination of the reststrahlen bands in garnets.

In comparing Tables I and II, we can see that there is a difference between the reststrahlen bands obtained from the Lorentz oscillator and from the Kurosawa formula. Since the calculation of the Kurosawa formula using Eq. (1) neglects the contribution of the damping effect, i.e., the difference due to the damping, it suggests that the reststrahlen band can be localized within 0.1 cm^{-1} in instances where the damping effect can be removed completely. The value for this is equal to 3 GHz, which is close to that obtained by theoretical calculation using MD theory for $Dy_3Al_5O_{12}$ ($\omega_{\mathrm{TO}} = 99.4$ cm^{-1} and $\omega_{\mathrm{LO}} = 99.6$ cm^{-1}) [7]. However, in reality the bulk crystals include various damping factors related to the anharmonic decay of optical phonons into two acoustic phonons [16], and the scattering induced at crystal defects [16–18]. Consequently, the FWHM derived from the Lorentz oscillator model should be considered when applying the results to band-reflection devices [Table I]. This reveals that a linewidth of 3.42 cm^{-1} corresponds to 100 GHz, which is narrower than that of current bandpass filters ($\Delta f = 300$ GHz) [3].

It has been previously reported that the frequency peaks of optical phonons in the IR region are associated with the lattice constant [19]. In an effort to ascertain the precise correlation between dielectric absorption and the lattice constant, the peak frequencies of $Y_3Fe_5O_{12}$ (YIG) and $Ho_3Fe_5O_{12}$ (HoIG) were studied as a typical example. As shown in Fig. 3, the peak position of YIG shifts to a higher frequency than that of HoIG. This is despite the fact that the similarity in bond length between rare-earth and oxygen ions in garnets means that the

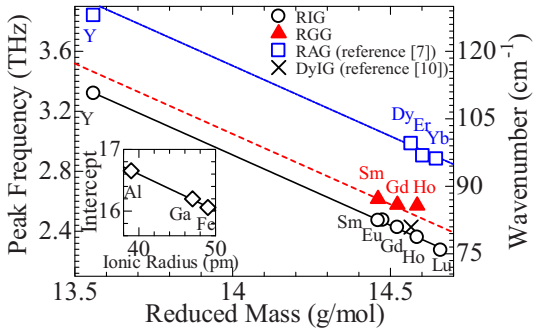

FIG. 3. (Color online) The dependence of dielectric absorption frequency on the reduced mass.

two have very similar lattice constants. This is also true of the bond length between the metal and oxygen ions [20]; thus, the frequency shift between YIG and HoIG cannot be explained in terms of the lattice parameter.

The shift in peak frequency can, however, be described as a function of the reduced mass of the R site (Fig. 3). Furthermore, the M sites occupied by Ga, Al, and Fe ions also play an important role in controlling the peak frequency, the peak position being gradually shifted to a higher frequency in the order of Al > Ga > Fe. This tendency can also be applied to the relationship between the ionic radius of the M sites and frequency shift. Given that the ionic radius is related to the strength of an ionic bond, as described by the change in the spring constant, the peak frequency (ω_p) changes linearly in relation to the reduced mass and ionic radius of the R and M sites, respectively. This relation is given by the following expression:

$$\omega_p = \alpha\delta + \beta r_{\text{ion}} + \omega_0, \tag{5}$$

where α and β are -0.94 and -0.0588, respectively, ω_0 is a constant value of 18.9 THz, δ (g/mol) is the reduced mass of the R sites, and r_{ion} (Å) is the ionic radius of the M sites.

Verification of this relationship was achieved using $Lu_3Sc_5O_{12}$, Lu ions having the greatest mass of rare-earth ions and Sc ions having the largest ionic radius. According to Eq. (5), the estimated peak frequency of $Lu_3Sc_5O_{12}$ is 0.754 THz, which is consistent with that of the experimental result (0.750 THz). Therefore, the peak position of the reststrahlen band in a garnet system can be theoretically estimated using the two parameters of δ and r_{ion}. This finding provides opportunities to fabricate practical optical devices based on the reststrahlen bands of garnets in the THz regime.

IV. CONCLUSION

Through this investigation into the reststrahlen bands of garnets, it has been found that the intensity of dielectric absorption in the THz regime is strongly dependent on crystal orientation and polarization direction. This is attributed to a restriction in the vibrational motion of rare-earth ions in GGG garnet, with a theoretical fit to the experimental data confirming that the phonon-polariton frequency at around 85.5 cm^{-1} exhibits a narrow linewidth of 100 GHz at RT. Finally, it has been demonstrated that the peak frequency can be manipulated by selectively changing the reduced mass and ionic radius of R and M sites, respectively.

ACKNOWLEDGMENT

The authors would like to thank Advantest Co. for the loan of the TAS7500SP device used in this study.

[1] D. H. Auston, K. P. Cheung, and P. R. Smith, Appl. Phys. Lett. **45**, 284 (1984).
[2] M. Tonouchi, Nat. Photonics **1**, 97 (2007).
[3] O. Paul, R. Beigang, and M. Rah, Opt. Express **17**, 18590 (2009).
[4] T. Hasebe, Y. Yamada, and H. Tabata, Jpn. J. Appl. Phys. **51**, 04DL03 (2012).
[5] H. J. Bakker, S. Hunsche, and H. Kurz, Phys. Rev. Lett. **69**, 2823 (1992).
[6] S. Kojima, N. Tsumura, M. W. Takeda, and S. Nishizawa, Phys. Rev. B **67**, 035102 (2003).
[7] K. Papagelis and S. Ves, J. Appl. Phys. **94**, 6491 (2003).
[8] T. J. Kane and R. L. Byer, Opt. Lett. **10**, 65 (1985).
[9] R. V. Mikhaylovskiy, E. Hendry, F. Y. Ogrin, and V. V. Kruglyak, Phys. Rev. B **87**, 094414 (2013).
[10] T. D. Kang, E. C. Standard, P. D. Rogers, K. H. Ahn, A. A. Sirenko, A. Dubroka, C. Bernhard, S. Park, Y. J. Choi, and S. W. Cheong, Phys. Rev. B **86**, 144112 (2012).
[11] T. Kurosawa, J. Phys. Soc. Jpn. **16**, 1298 (1961).
[12] R. H. Lyddane, R. G. Sachs, and E. Teller, Phys. Rev. **59**, 673 (1941).
[13] W. Cochran and R. A. Cowley, J. Phys. Chem. Solids **23**, 447 (1962).
[14] K. Lal and H. K. Jhans, J. Phys. C: Solid State Phys. **10**, 1315 (1977).
[15] A. I. Belyaeva, A. A. Galuza, and A. D. Kudlenko, Semicond. Phys. Quantum Electron. Optoelectron. **6**, 81 (2003).
[16] U. T. Schwarz and M. Maier, Phys. Rev. B **53**, 5074 (1996).
[17] B. Bittner, M. Scherm, T. Schoedl, T. Tyroller, U. T. Schwarzl, and M. Maier, J. Phys.: Condens. Matter **14**, 9013 (2002).
[18] S. Kojima, Jpn. J. Appl. Phys. **32**, 4373 (1993).
[19] N. T. McDevitt, J. Opt. Soc. Am. **59**, 1240 (1969).
[20] F. Eular and J. A. Bruce, Acta Crystallogr. **19**, 971 (1965).